AFRL-RB-WP-TR-2009-3057

STOCHASTIC NONLINEAR AEROELASTICITY

Philip S. Beran, Ned J. Lindsley, José Camberos, and Mohammad Kurdi

Design and Analysis Methods Branch
Structures Division

JANUARY 2009
Final Report

AIR FORCE RESEARCH LABORATORY
AIR VEHICLES DIRECTORATE
WRIGHT-PATTERSON AIR FORCE BASE, OH 45433-7542
AIR FORCE MATERIEL COMMAND
UNITED STATES AIR FORCE

NOTICE AND SIGNATURE PAGE

AFRL-RB-WP-TR-2009-3057 HAS BEEN REVIEWED AND IS APPROVED FOR PUBLICATION IN ACCORDANCE WITH ASSIGNED DISTRIBUTION STATEMENT.

*//Signature//

PHILIP S. BERAN
Principal Research Aerospace Engineer
Design and Analysis Methods Branch
Structures Division

//Signature//

DENIS P. MROZINSKI
Chief
Design and Analysis Methods Branch
Structures Division

//Signature//

DAVID M. PRATT
Technical Advisor
Structures Division
Air Vehicles Directorate

*Disseminated copies will show "//Signature//" stamped or typed above the signature blocks.

REPORT DOCUMENTATION PAGE			*Form Approved* *OMB No. 0704-0188*

1. REPORT DATE ***(DD-MM-YY)***	**2. REPORT TYPE**	**3. DATES COVERED** ***(From - To)***
January 2009	Final	05 May 2004 – 23 January 2009

4. TITLE AND SUBTITLE STOCHASTIC NONLINEAR AEROELASTICITY	**5a. CONTRACT NUMBER** In-house
	5b. GRANT NUMBER
	5c. PROGRAM ELEMENT NUMBER 0601102
6. AUTHOR(S) Philip S. Beran, Ned J. Lindsley, José Camberos, and Mohammad Kurdi	**5d. PROJECT NUMBER** A03K
	5e. TASK NUMBER
	5f. WORK UNIT NUMBER 0A
7. PERFORMING ORGANIZATION NAME(S) AND ADDRESS(ES) Design and Analysis Methods Branch (AFRL/RBSD) Structures Division, Air Force Research Laboratory Air Vehicles Directorate Wright-Patterson Air Force Base, OH 45433-7542 Air Force Materiel Command, United States Air Force	**8. PERFORMING ORGANIZATION REPORT NUMBER** AFRL-RB-WP-TR-2009-3057
9. SPONSORING/MONITORING AGENCY NAME(S) AND ADDRESS(ES) Air Force Research Laboratory Air Vehicles Directorate Wright-Patterson Air Force Base, OH 45433-7542 Air Force Materiel Command United States Air Force	**10. SPONSORING/MONITORING AGENCY ACRONYM(S)** AFRL/RBSD
	11. SPONSORING/MONITORING AGENCY REPORT NUMBER(S) AFRL-RB-WP-TR-2009-3057

12. DISTRIBUTION/AVAILABILITY STATEMENT
Approved for public release; distribution unlimited.

13. SUPPLEMENTARY NOTES
PAO Case Number: 88ABW 2009-0448, 12 Feb 2009. Report contains color.

14. ABSTRACT
This report documents the culmination of in-house work in the area of uncertainty quantification and probabilistic techniques for aeroelasticity. The work was divided into different project areas, including: accurate analysis of limit-cycle oscillations for simple aeroelastic systems with variability; probabilistic prediction of flutter in systems with distributed variability (random fields); optimization of nonlinear dynamic systems (deterministic with intent to transition to risk-quantified optimization), and incorporation of sensitivities into probabilistic analyses. Technology developed in this task is being transitioned in the STOFAM program and extended in the new laboratory task “Risk-Based Computational Prototyping.”

15. SUBJECT TERMS
uncertainty quantification, non-deterministic techniques, reduced order modeling, stochastic bifurcation, micro-air vehicles, limit-cycle oscillation

16. SECURITY CLASSIFICATION OF:			**17. LIMITATION OF ABSTRACT:**	**18. NUMBER OF PAGES**	**19a. NAME OF RESPONSIBLE PERSON** (Monitor)
a. REPORT	**b. ABSTRACT**	**c. THIS PAGE**			Philip S. Beran
Unclassified	Unclassified	Unclassified	SAR	44	**19b. TELEPHONE NUMBER** *(Include Area Code)* N/A

Standard Form 298 (Rev. 8-98)
Prescribed by ANSI Std. Z39-18

STOCHASTIC NONLINEAR AEROELASTICITY

Philip S. Beran, Ned J Lindsley, José Camberos, and Mohammad Kurdi

Air Force Research Laboratory, Air Vehicles Directorate

WPAFB, OH

Abstract

The main purpose of the research was to develop new computational methods for treating nonlinear, dynamic, aeroelastic interactions at the design level. We considered two classes of problems requiring these methods: (1) reliability based design optimization and/or certification of fixed wing aircraft susceptible to nonlinear oscillations (for the purpose of avoiding dangerous oscillations), and (2) multidisciplinary design optimization of flapping wing actuation for micro air vehicles (for the purpose of exploiting favorable oscillations). In the former class of problems, we wish to estimate the probability that an air vehicle will fail to an aeroelastic event of sufficient severity. This capability would enable flight-test engineers to more effectively use scarce test resources and more rigorously frame clearance recommendations (e.g., accounting for variability in tested equipment, such as store properties). These methods will also provide the designers of future air vehicles new techniques by which reliability can be addressed early in the design process, thereby lowering system development and testing costs. In the latter class of problems, we explore the multidisciplinary optimization of dynamic systems using the adjoint-variable approach. This capability would enable the power-efficient, time-dependent actuation of nonlinear systems, tailored to aerodynamic loads that arise in response to structural actuation. To make progress, we are conducting research in the following areas: (1) developing gradient-based optimization procedures for computing minimum work actuations of linear and nonlinear systems using analytical sensitivities [completed work]; (2) extending these procedures for addressing the robustness of designs to uncertain actuations and loadings; (3) developing low-discrepancy samples for high-dimensional spaces; (4) developing a framework for computing solution ensembles for complex aircraft, and (5) developing techniques for fast construction and use of surrogate models for structures with distributed variability.

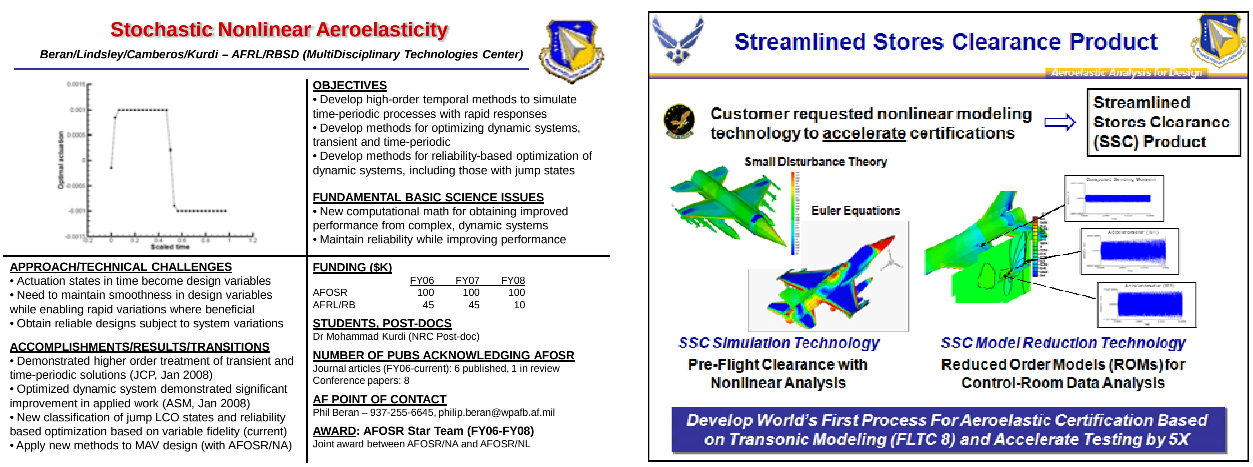

Figure 1: Overview of research activity (left; 2008 Spring Review); Transition of reduced order modeling technology to flight-test program for aeroelastic certification (right).

Summary

Figure 1 (left) describes the research objectives, technical challenges, and task accomplishments. It is noted that this task forms a broader collaboration with a task entitled "Physics-Based Design of Micro Air Vehicles" (AFOSR/NA). The summary slide taken from the AFOSR 2008 Spring Review shows a significant result, which is the actuation time history of a linear, mechanical system optimized for minimum work. The time-periodic actuation is like that of a square wave, demonstrating the need for the methodology to accommodate rapid transitions. We believe this is a desirable capability for optimizing the kinematics of micro air vehicles. Recent work has focused on the optimal actuation of nonlinear systems. In this document, we: (1) summarize our actuation optimization of both linear and nonlinear dynamic systems; (2) discuss recent progress in the development of smart, low-discrepancy, sampling strategies for higher dimensional spaces, and (3) overview a framework we are building to enable the sampling of the solution space of large, aerospace systems. Current activity in (1) generating stochastic, time-periodic forcing functions for the robust actuation of dynamic systems, and (2) assessing uncertain flutter speeds for structures with distributed variability[9], will be discussed at the grantees' meeting.

Figure 1 (right) describes how reduced order modeling technology developed in the combined tasks has been transition to the Streamlined Stores Clearance Product, which is now in flight-test validation. This goal of this Product is to reduce the amount of testing needed to certify wing/stores for aeroelastic safety.

Gradient-Based Optimization of Linear and Nonlinear Dynamic Systems. During the FY06-FY08 grant period, an *hp*-Cyclic technique was developed for efficiently computing time-periodic solutions in the presence of high-frequency content[5]. This approach is judged to be beneficial for MAV stroke patterns containing rapid transitions in wing orientation and stroke direction. The foundation for the technique is the *p*-order spectral element. We consider problems of the form

$$\frac{d\mathbf{x}}{dt} + \mathbf{A}\mathbf{x} = \mathbf{f}(\mathbf{x}) + \mathbf{c}(t),$$

where **x** is an n-dimensional vector, **A** is a square matrix of rank n, **f** is a nonlinear function of **x**, and **c** is an actuation dependent on time. The variables $\mathbf{x}(t)$ correspond to the collocation of the various values of a continuous function $x(t)$ evaluated at discrete points. For time-periodic analysis, with period T, we enforce $\mathbf{x}(t+T) = \mathbf{x}(t)$. Following discretization in time with spectral elements, and enforcement of the periodicity condition, a system of the form $\mathbf{L}_{\mathrm{g}}\mathbf{X}_{\mathrm{g}} = \mathbf{A}_{\mathrm{g}}\mathbf{X}_{\mathrm{g}} - \mathbf{L}_{\omega\mathrm{g}}\mathbf{F}_{\mathrm{g}} - \mathbf{L}_{\omega\mathrm{g}}\mathbf{C}_{\mathrm{g}}$ is obtained, where the expanded vector $\mathbf{X}_{\mathrm{g}}$ represents all variables at all times. Sensitivities of monolithic-time solutions were computed via the adjoint method (as well as finite differences and the direct method) and used in a design optimization process. An appropriate objective function, $I(\lambda)$, is identified, and relevant design variables, λ, considered. Sensitivities (considering dependence of A on the design variables) satisfy

$$\frac{\partial I}{\partial \lambda_i} = \frac{\partial I}{\partial \mathbf{X}_{\mathrm{g}}}^{\mathrm{T}} \frac{\partial \mathbf{X}_{\mathrm{g}}}{\partial \lambda_i} = \frac{\partial I}{\partial \mathbf{X}_{\mathrm{g}}}^{\mathrm{T}} \left[\mathbf{L}_{\mathrm{g}} - \mathbf{A}_{\mathbf{g}} + \mathbf{L}_{\omega\mathrm{g}} \frac{\partial \mathbf{F}_{\mathrm{g}}}{\partial \mathbf{X}_{\mathrm{g}}} \right]^{-1} \frac{\partial \mathbf{A}_{\mathrm{g}}}{\partial \lambda_i} \mathbf{X}_{\mathrm{g}},$$

which is efficiently computed by pre-computing Ψ (for relatively few constraints):

$$\Psi^{\mathrm{T}} \equiv \frac{\partial I}{\partial \mathbf{X}_{\mathrm{g}}}^{\mathrm{T}} \left[\mathbf{L}_{\mathrm{g}} - \mathbf{A}_{\mathbf{g}} + \mathbf{L}_{\omega\mathrm{g}} \frac{\partial \mathbf{F}_{\mathrm{g}}}{\partial \mathbf{X}_{\mathrm{g}}} \right]^{-1}.$$

We applied the monolithic-time sensitivity analysis procedure to two problems: a linear oscillator driven by a time-periodic actuation and the same oscillator with nonlinear contributions to stiffness. Different targets of peak displacement were examined. The actuation trajectory was defined by a set of cubic splines on a fixed, finely spaced grid of temporal points. The optimization was performed with MATLAB's sequential quadratic programming capability, with sensitivities supplied by the procedure described above. The design variables are period of actuation (*T*) and the values of actuation force at the ends of each spline element. For smaller values of peak displacement, the period of actuation was found to depart from the natural period by around 10%. The optimized actuation was such that, on an equivalent work basis, 25% more displacement of the system mass was achieved. A sample of optimized actuation forces is shown in Figure 2 for a target displacement of 2.5.

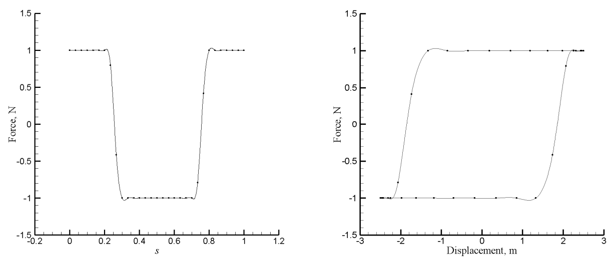

Figure 2: Actuation forces versus scaled time (left) and displacement (right).[8]

The optimal actuation of a modified Duffing equation was also studied, which contained cubic and pentic contributions to the stiffness term:

$$\frac{1}{T^2}\ddot{x}_{ca} + \frac{2}{T}\zeta\omega_n\dot{x}_{ca} + \omega_n^2(x + \beta x_{ca}^3 + \gamma x_{ca}^5) = \frac{a}{m}f(s)$$

Sensitivity results are shown in Figure 3 (linear and cubic stiffness only), which show that sensitivities for multiple solutions are accurately captured with the adjoint-variable approach.

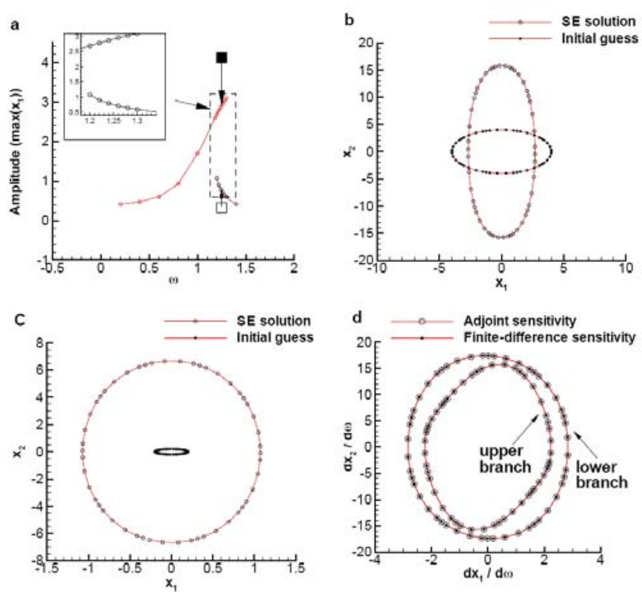

Figure 3: Sensitivities of solutions of the Duffing equation to variations in actuation frequency.[7]

Development of Smart, Low-Discrepancy Sampling (LDS) Methods. Quasi-Monte Carlo (QMC) integration is the same in form as conventional Monte Carlo (MC) integration except that quasi-random numbers (sequences, samples) can be used instead of pseudo-random numbers. It is already well known that QMC integration is more efficient than MC integration, as proved by the Koksma–Hlawaka inequality. Furthermore, there are classes of quasi-random sequences that require sophisticated mathematical constructs (matrices and polynomials of a certain combinatorial nature over finite fields) to achieve optimal performance with respect to QMC integration. The associated portable, efficient parallel libraries are being tested in this task[3]. Exploratory results have demonstrated significant improvement in convergence and accuracy using low-discrepancy sequences for Monte-Carlo numerical integration. The results of our tests in one particular area demonstrated that the use of quasi-random numbers were superior to the standard pseudo-random generators commonly used. We showed that for complicated multidimensional integrals, the new method improved the quality of the results while using fewer integration points (Figure 4). We believe that the techniques have a wide-range of applications.

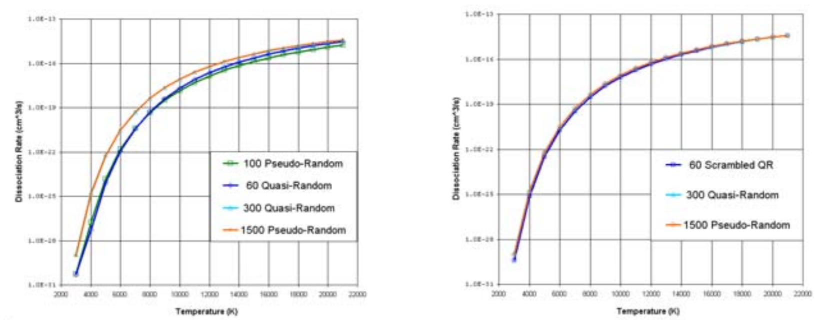

Figure 4: Comparison of MC and QMC methods applied to calculating O_2−*Ar* dissociation rates: Baseline comparison with 1500 MC points (left) and comparison using optimally selected LDS (right).

We performed a preliminary assessment of QMC integration to the computation of failure probability for an aeroelastic airfoil. Probability of failure was computed with MC and QMC integration at an optimum point found by Missoum *et al*. in a reliability based optimization of the properties of the airfoil's structural support[10]. Missoum used the Support Vector Machine algorithm to classify the failure surface. Any random sample was considered to "fail" if the SVM function, *s*, returned a positive value. The parameters (initial angle of attack, pitch cubic stiffness, and pitch pentic stiffness) where assumed to be uniform random variables. Results obtained with MC and QMC integration are compared in Figure 5 (left). The number of samples needed to yield converged integration results is about the same: O(10^5).

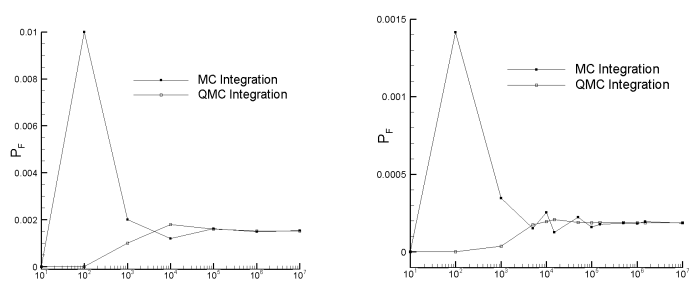

Figure 5: Probability of failure estimates obtained with MC and QMC integration: discrete failure surface (left) and smoothed failure surface (right).

We then re-examined the definition of failure built into the SVM procedure that was used to construct the failure surface. The SVM function, *s*, varies smoothly within a margin where no samples lie. Thus, for the level of sampling carried out in the construction of the failure surface, the true location of the failure surface is indeterminate: it can lie anywhere in the SVM margin. In this sense, the assignment of failure at $s = 0$ is strictly a numerical approximation. Now, realizing that the failure surface does not need to be represented precisely, we exploit the smoothness the SVM function within the margin to weight contributions of samples in this region during the numerical integration. In this way, we constructed an integrand taking values of +1 or – 1 outside the margin and values that linearly varied within the margin.

With the integrand now C^0-continuous, we then repeated our comparison of MC and QMC integration, recording results in Figure 5 (right). In this figure, it is clearly seen that QMC converges faster than MC integration, perhaps achieving a useful result with an order of magnitude fewer samples. *We fully expect that in a space of dimension larger than 3, the comparison between MC and QMC will favor QMC integration more.* We also note that the failure probability computed with both techniques is different from that shown in Figure 5 (left). We attribute this difference to the need to create the SVM with a greater number of samples to reduce the margin width.

Construction of Framework for Solution Space Sampling of Aerospace Systems. We developed a probabilistic representation of a wing/box structure, assigning variability to structural stiffness and mass properties. This model is used to compute ensembles of flutter speed for linear[1,6] and nonlinear aerodynamics (1000 samples). Results are summarized in Figure 6 below using transonic small-disturbance theory. We are in the process of replacing the aerodynamic solver based on small-disturbance theory with a new aerodynamic solver based on a Cartesian Euler methodology (developed by ZONA Technology Inc.). The new capability provides superior convergence, works well for supersonic cases, and is suitable for analyzing trimmed, complex configurations, like those we have recently studied. See Figure 7.

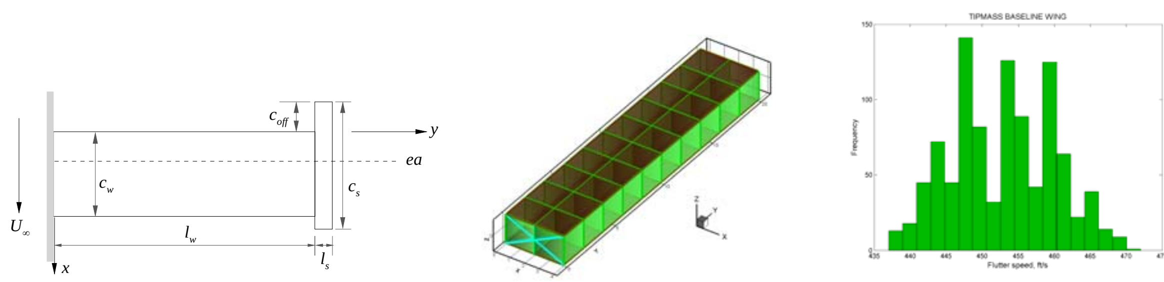

Figure 6: Wing and store geometry (left), wing box structural model (middle), flutter distribution (right).

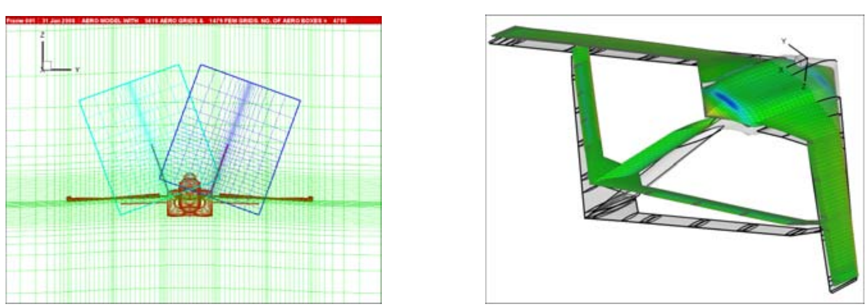

Figure 7: Aeroelastic analysis of realistic aircraft: X-53 (left) and SensorCraft (right; trimmed).

Acknowledgment/Disclaimer

This work was sponsored (in part) by the Air Force Office of Scientific Research, USAF, under LRIR 03VA01COR. The views and conclusions contained herein are those of the authors and should not be interpreted as necessarily representing the official policies or endorsements, either expressed or implied, of the Air Force Office of Scientific Research or the U.S. Government.

References and Recent Publications

1. Beran, P., Badcock, K., Woodgate, M., Kurdi, M., Lindsley, N., Myers, A., and Pettit, C., "A Multi-Fidelity Framework for Quantification of Uncertainty in Aeroelastic Systems," RTO AVT-147 Symposium on Computational Uncertainty, Athens, Paper A-71, Dec. 2007.
2. Beran, P., Kurdi, M., Lindsley, N., and Camberos, J., "A Review of Uncertainty Quantification Concepts for Aerospace Systems," Invited Presentation, AIAA ASM Conference, Jan 2009.
3. Camberos, J., Greendyke, R.B., and Lambe, L.A., "On Direct Simulation Quasi-Monte Carlo Methods," 40th AIAA Thermophysics Conference, Seattle WA, June 2008.
4. Hajj, M., and Beran, P., "Identification of Nonlinearities Responsible for Limit Cycle Oscillations of Fighter Aircraft," *Journal of Aircraft* [accepted for publication].
5. Kurdi, M., and Beran, P., "Spectral Element Method in Time for Rapidly Actuated Systems," *Journal of Computational Physics*, Vol. 227, No. 3, 2008, pp. 1809-1835.
6. Kurdi, M., Lindsley, N., and Beran, P., "Uncertainty Quantification of Flutter Boundary in Goland+ Wing," AIAA 2007-6309, August 2007.
7. Kurdi, M., Beran, P.S., and Snyder, R.D., "Work-Amplitude Optimal Actuation of a Nonlinear Resonant System," submitted to *Structural and Multidisciplinary Optimization*.
8. Kurdi, M., and Beran, P., "Optimization of Dynamic Response Using Spectral Element Method in Time," AIAA 2008-0903, January 2008, and submitted to *Structural and Multidisciplinary Optimization*.
9. Lindsley, N., Kurdi, M., and Beran, P., "Methods for Quantifying Uncertainties in Aeroelastic Responses," RTO AVT-147 Symposium on Computational Uncertainty, Paper A-62, Athens, Dec. 2007.
10. Missoum, S., Beran, P., Kurdi, M., and McFarland, M., "Reliability-based design optimization of nonlinear aeroelastic problems," AIAA 2008-2075, April 2008.
11. Pettit, C.L., Hajj, M., and Beran, P.S. "Gust Loads with Uncertainty Due to Imprecise Gust Velocity Spectra," AIAA 2007-1965 and submitted to *Journal of Fluids and Structures*.

Personnel Supported During Duration of Grant: Dr. Philip S. Beran, Principal Research Aerospace Engineer, AFRL/RBSD; Dr. Ned J Lindsley, Aerospace Engineer, AFRL/RBSD; Dr. José Camberos, AFRL/RBSD**;** Dr. Mohammad Kurdi, AFRL/RBSD (NRC contractor, fully dedicated to this lab task).

Honors & Awards Received: AFOSR Star Team Award, 2006-2008.

AFRL Point of Contact: Dr. Philip Beran, AFRL/RBSD, WPAFB, OH, Phone 937-255-6645.

Transitions: Stochastic Nonlinear Aeroelasticity is an enabling technology for the Streamlined Stores Clearance Product – Dr. Beran, Product Manager.

New Discoveries: No patents awarded.

Appendix. Results of a detailed nature are documented in the following pages.

Goals

- Review non-deterministic approaches from the perspective of aeroelasticity and certification
  - What new challenges are encountered?
  - Do not assume background in probabilistic techniques
- Re-examine aeroelastic analysis from the perspective of non-deterministic approaches
  - Do not assume background in aeroelasticity
- Use sample problems
  - Generic (educational)
  - Not-so generic (industrial)
- Theme: use of aeroelastic sensitivities

2

Some Resources

- *Introduction to Non-Deterministic Approaches*, An AIAA Professional Series Course developed by the AIAA Non-Deterministic Approaches Technical Committee (Enright, Grandhi, Mahadevan, Thacker)
- Review Article – Chris Pettit, "Uncertainty Quantification in Aeroelasticity: Recent Results and Research Challenges," *Journal of Aircraft*, Sep-Oct, 2004.
- Recent Article – Hosder, Walters and Balch, "Efficient Uncertainty Quantification Applied to the Aeroelastic Analysis of a Transonic Wing," AIAA 2008-729.

3

Outline

- Preliminaries
  - Aeroelastic failure mechanism: flutter
  - Sources of variability
  - Elements of probability theory
- Probabilistic view of flutter
  - Numerical challenges: indirect vs direct
  - Sample flutter problem (linear)
  - Monte Carlo simulation and probability of failure
- Techniques and applications
  - Surrogate models of failure surfaces
  - Surrogate physical models
  - Improved sampling

4

Flutter

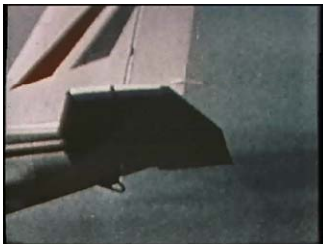

Flutter is a divergent and catastrophic interaction between a structure and the surrounding airstream (aerodynamic, inertial, and elastic forces)

Must meet a flutter certification requirement

5

Sources of Uncertainty

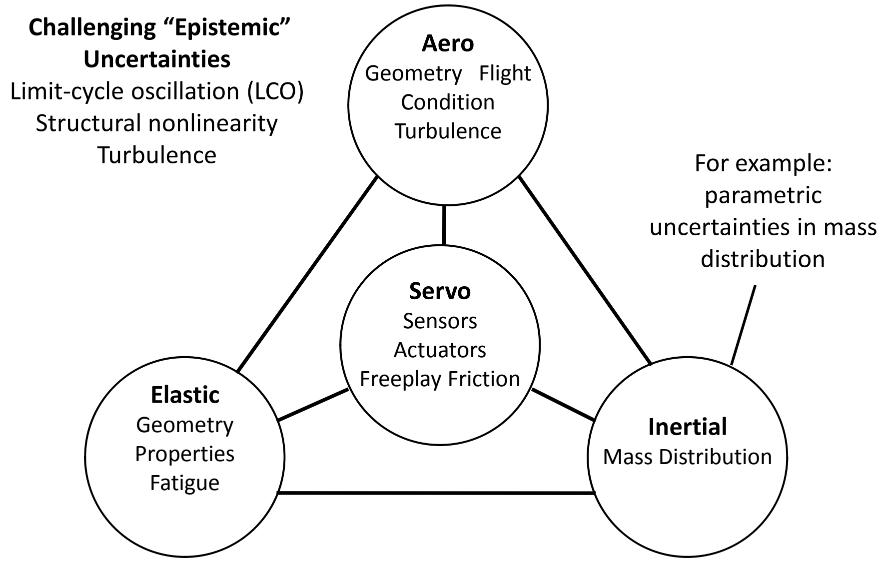

6

Sources of Uncertainty (cont.): Pitt et al.

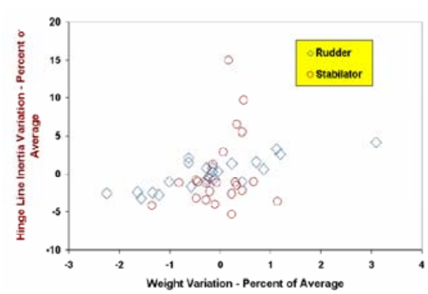

Figure 2. Hinge Line Inertia Variation For Rudder and Stabilator as a Function of Weight Variation.

Figure 3. Frequency Variation on Measured Mode Shapes on One Test Aircraft.

Pitt, Haudrich and Thomas, "Probabilistic Aeroelastic Analysis and Its Implications on Flutter Margin Requirements," AIAA 2008-2198.

7

AIAA NDA Probability and Statistics Fundamentals (Michael Enright)

Discrete Random Variables

– Let X be a discrete random variable, then…

$$f_X(x_k) = P(X = x_k)$$

Probability Mass Function

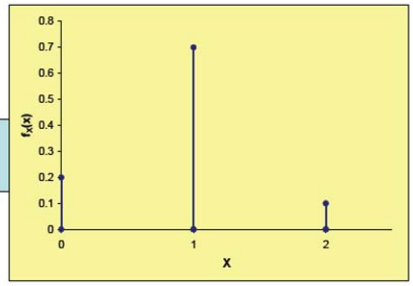

$$F_X(x_k) = P(X \le x_k)$$

Cumulative Mass Function

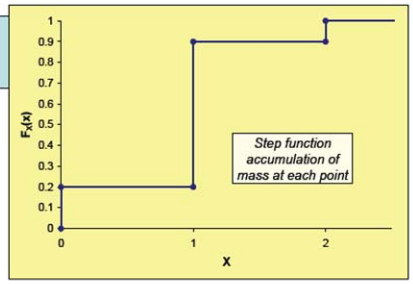

where

$$0 \le P(X = x_i) \le 1$$

$$P(X \le x_k) = \sum_{1}^{k} P(X = x_i)$$

$$\sum_{i} P(X = x_i) = 1$$

8

AIAA NDA, Enright (cont.)

Continuous Random Variables

– Let X be a continuous random variable, then…

$$f_X(x)$$

Probability Density Function (PDF)

Use p(x) to denote PDF

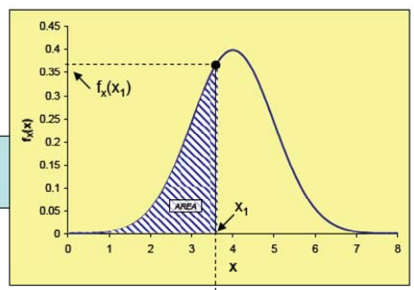

$$F_X(x) = P(X \le x)$$

Cumulative Density Function (CDF)

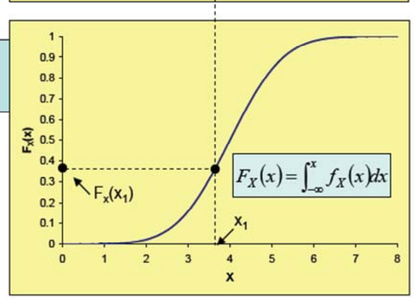

where

$$f_X(x) = \frac{dF_X(x)}{dx} \ge 0 \quad \text{PDF and CDF are related}$$

$$\int_{-\infty}^{\infty} f_X(x)dx = 1$$

9

More Essentials

Mean (not to be confused with mass ratio)

Expected value

$$\mu = E[x] = \sum_{i=1}^{n} x_i p(x_i) \quad \text{discrete}$$

$$\mu = E[x] = \int_{-\infty}^{\infty} x p(x) dx \quad \text{continuous}$$

$$V = E[(x-\mu)^2] = \int_{-\infty}^{\infty} (x-\mu)^2 p(x) dx$$

Variance ($\sigma = V^{1/2}$ = standard deviation)

$$p(x) = \frac{1}{\sigma\sqrt{2\pi}} e^{-(x-\mu)^2/2\sigma^2}$$

Gaussian PDF

p(x) AIAA NDA, Enright

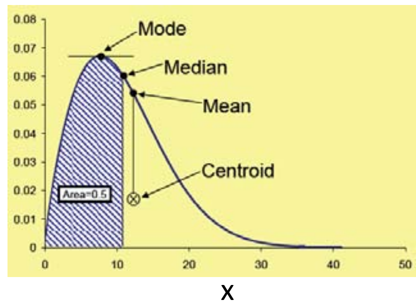

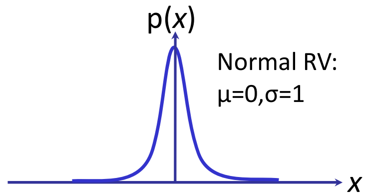

Probabilistic View of Flutter

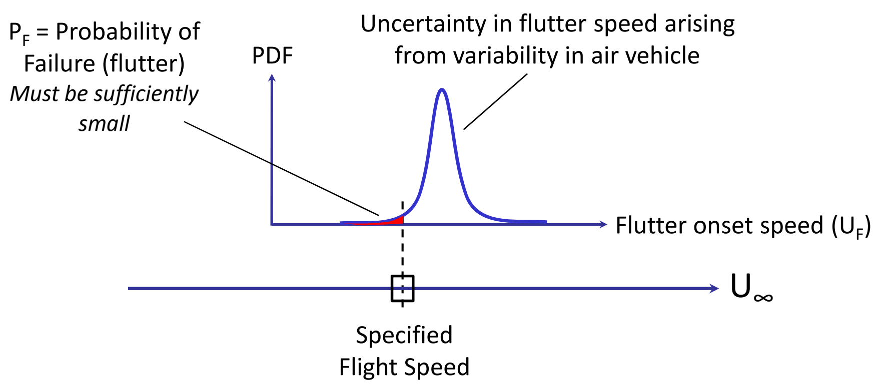

Members of the same air vehicle class have different flutter speeds

Comparison

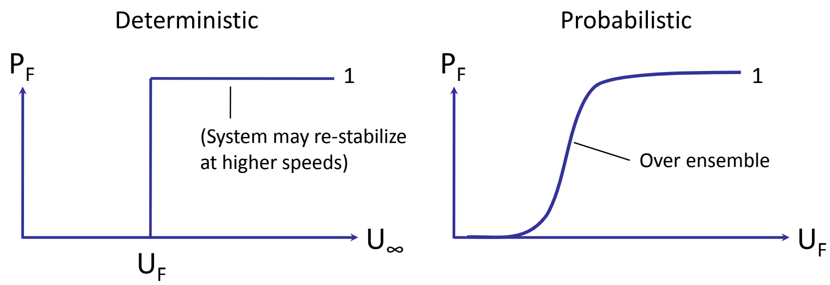

Linear Aeroelastic Proto-Problem

- Pitch and plunge structural coupling of a rigid airfoil ("typical section")
- Linear aerodynamics and structural dynamics
- Time-domain formulation

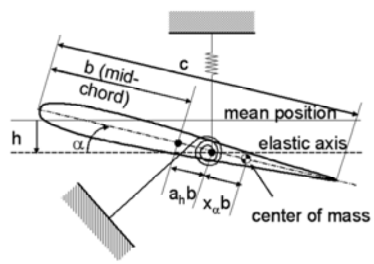

Frequency ratio (plunge/pitch)

$$\ddot{y} + x_\alpha \ddot{\alpha} + \left(\frac{\omega}{U}\right)^2 y = -\frac{1}{\pi\mu} C_L \qquad \frac{x_\alpha}{r_\alpha^2}\ddot{y} + \ddot{\alpha} + \frac{1}{U^2}\alpha = \frac{2}{\pi\mu r_\alpha^2} C_M$$

h/b

Mass center offset

Mass ratio

Reduced velocity ($U_\infty/(\omega_\alpha b)$)

Force and moment coefficients (modeled)

Determining Flutter Speed (Simulation)

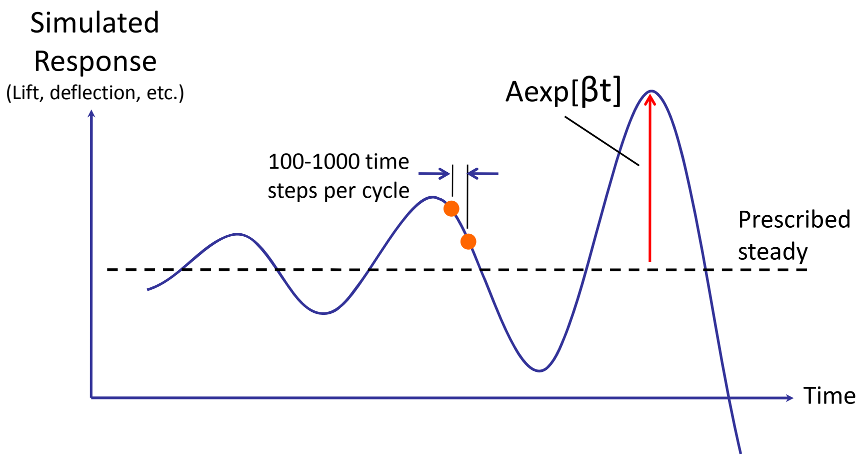

Stability of single system is observed by costly time-accurate simulation

14

Governing Equations and the Jacobian, J

- Arrange the dependent variables in the vector x
- Arrange the parameters in the vector λ
- Arrange the nonlinear governing equations in the first-order system

$$\frac{dx}{dt} = F(x;\lambda) \qquad \text{(N=8 equations)}$$

- F is linearized with the N-by-N Jacobian matrix

$$J = \left[\frac{\partial F_i}{\partial x_j}\right] \qquad \frac{dx}{dt} = J(\lambda)x \qquad \text{Eigenvalues } \beta$$

15

Indirect Approach Introduces Uncertainty

Goal: Determine U_F such that $g = \max(\mathrm{Re}(\beta(U))) = 0$

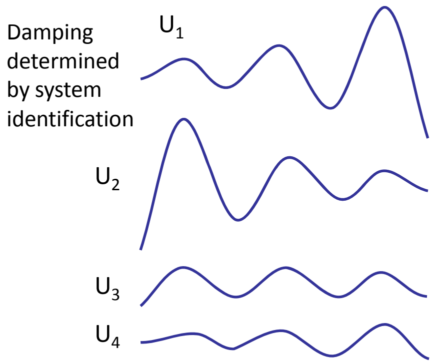

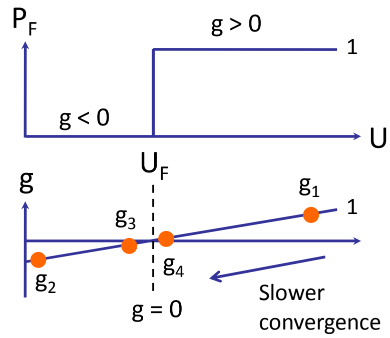

"Bracketed" flutter speed is uncertain: $U_3 < U_F < U_4$

16

Direct Approach Removes Uncertainty

- Satisfy $g = \max(\mathrm{Re}(\beta(U))) = 0$ directly
  - Small systems: Newton's method + full system
  - Large systems: sparse-matrix techniques
- Nonlinear steady-state + linearized dynamics
- Dynamic analysis rendered in steady form

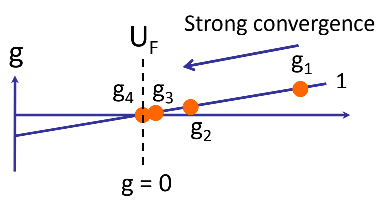

Flutter computations at cost of steady-state analysis

17

Critical Eigenvalues

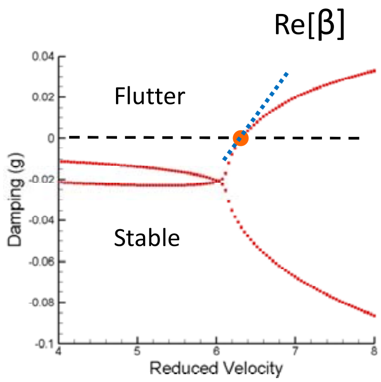

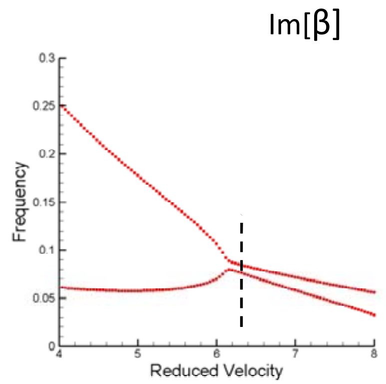

Eigenvalue problem is not linear

18

Parameter Variations

■ Baseline

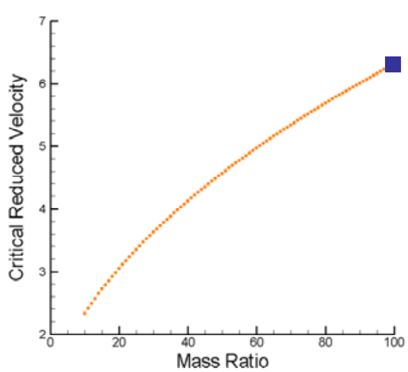

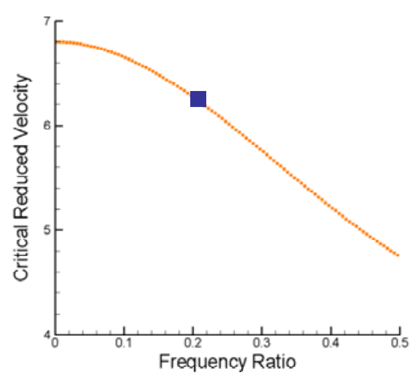

19

Sensitivity Analysis (Linear Variation)

- Want to compute *sensitivities of flutter speed* to parametric variations, $\partial U_F/\partial\lambda$
  - May have numerous parameters; determine most critical
  - Use to compute probability of failure
  - Use to compute flutter surfaces
- Avoid finite-difference approaches
  - $\partial U_F/\partial\lambda = [U_F(\lambda+\varepsilon) - U_F(\lambda)]/\varepsilon$
  - # of flutter computations proportional to # of parameters
  - Require high precision for each computation
- Employ a perturbation approach requiring only one precise flutter solution

20

Sensitivity Analysis Procedure

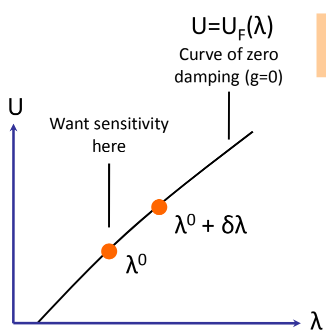

Goal: Compute $\partial U_F/\partial\lambda$ at known flutter point (λ^0, U_F)

$$\delta g = \frac{\partial g}{\partial U}\delta U + \frac{\partial g}{\partial \lambda}\delta\lambda = 0 \quad (U = U_F)$$

$$\frac{\partial U_F}{\partial \lambda} \cong -\underbrace{\left(\frac{\partial g}{\partial U}\right)^{-1}\frac{\partial g}{\partial \lambda}}_{\text{Need local sensitivities of damping}}$$

$$Jz = \beta z \quad (\lambda = \lambda^0)$$

$$(J+\delta J)(z+\delta z) = (\beta + \delta\beta)(z+\delta z)$$

Sensitivities of damping derived from eigenvalue perturbation analysis

21

Eigenvalue Perturbation Analysis

Goal: Compute δβ and use to compute damping sensitivity

$$(J+\delta J)(z+\delta z)=(\beta+\delta\beta)(z+\delta z)$$

Drop quadratic terms and drop Jz=βz

$$J\delta z+\delta J z=\beta\delta z+\delta\beta z$$

Need left & right eigenvectors corresponding to single flutter mode

$$q^*J\delta z+q^*\delta J z=\beta q^*\delta z+\delta\beta q^*z$$

$$q^*J=\beta q^* \quad (\lambda=\lambda^0)$$

$$q^*\delta J z=\delta\beta q^* z$$

Extract eigenvalue variation corresponding to flutter (g)

$$\frac{\delta\beta}{\delta\lambda}=\left[\frac{1}{q^*z}\right]\left[q^*\frac{\delta J}{\delta\lambda}z\right]$$

Compute with finite differences at low cost

ZAERO Theoretical Manual, ZONA Technology Inc. 2008

22

Comparisons

- Finite Difference
  - Sensitivity to mass ratio = 0.02978
  - Sensitivity to frequency ratio = -4.669
  - Sensitivity to cg = -9.892
- Analytical
  - Sensitivity to mass ratio = 0.02991
  - Sensitivity to frequency ratio = -4.638
  - Sensitivity to cg = -10.16

Computed sensitivities are in good agreement

23

Airfoil Failure Surface

Flutter surface is fairly linear over selected range

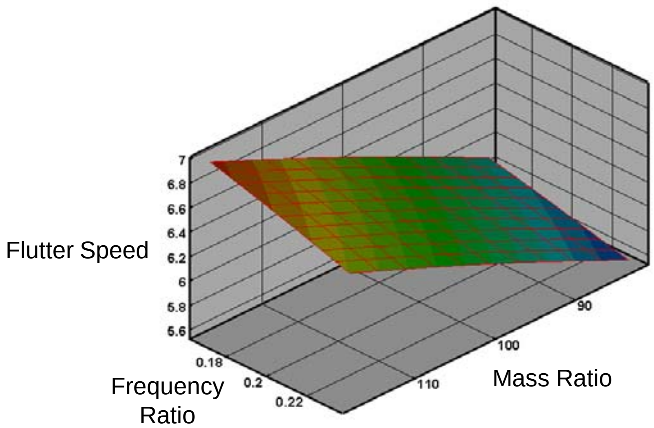

24

Monte Carlo Simulation

Goal: Learn by "Coin Flipping"

- Simulate many random events; interpret ensemble
- Convergence is slow (many samples – large N)
- Consider mass ratio and frequency ratio random
  - Pick distribution of interest
- Determine likelihood that airfoil fails (flutters)
  - Estimate probability of failure

$x_k \longrightarrow$ Model $\longrightarrow f_k$ $k = 1, \ldots, N$

25

AIAA NDA Monte Carlo Simulation (Thacker)

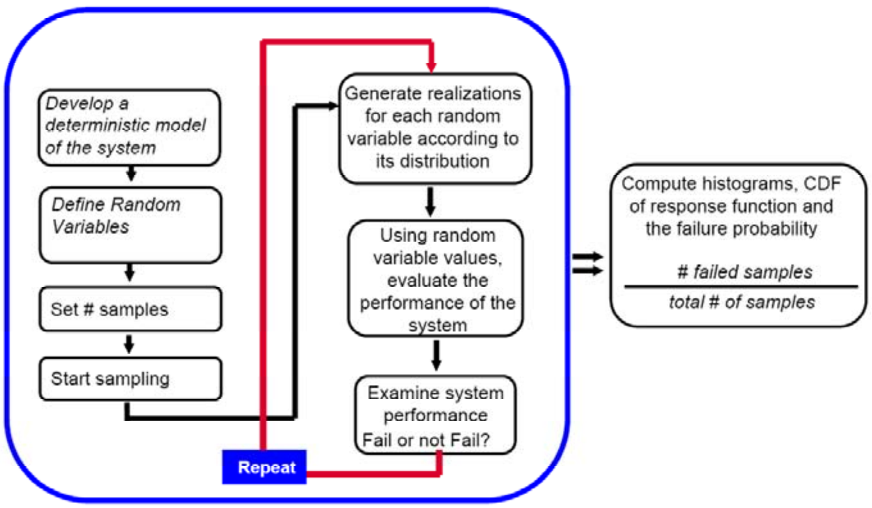

MCS: Gaussian and Uniform Distributions

COV = Standard Deviation/Mean

COV_μ=0.05
COV_ω=0.05

COV_μ=0.10
COV_ω=0.05

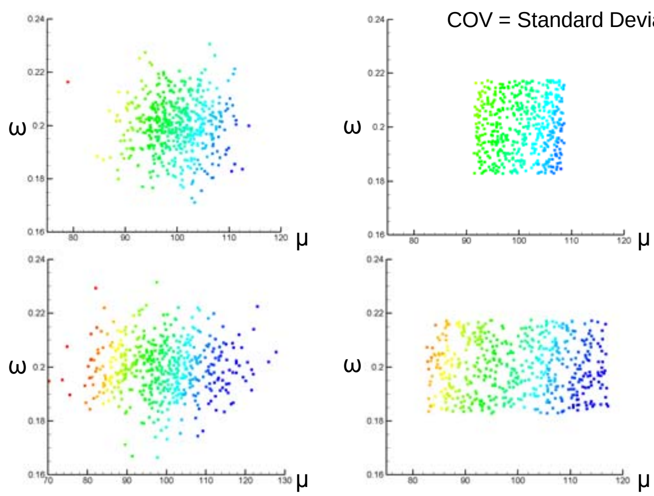

Choice of distribution simply determines sample locations

Probability of Failure (P_F)

P_F ~ # of failures / # of samples (U < 6)

Gaussian: 500 samples; 22 failures
$P_F = 0.044$ (5% COV)

Uniform: 500 samples; 125 failures
$P_F = 0.250$ (10% COV)

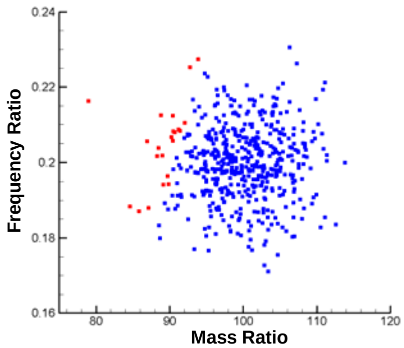

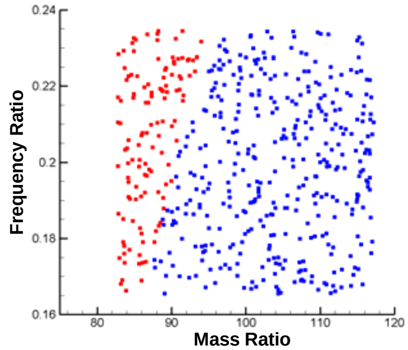

28

P_F for Linear Airfoil (cont.)

Convergence of Monte Carlo for different critical flutter speeds
(Gaussian distribution with COV=10%)

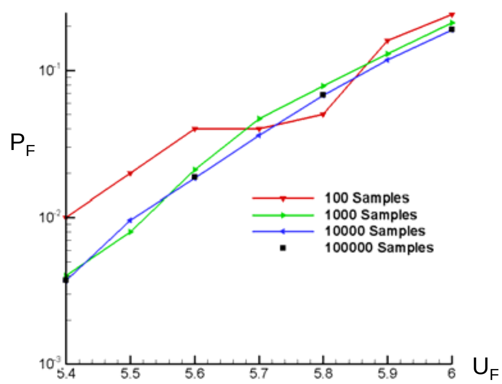

Monte Carlo is very costly if each collected sample is costly

29

How to Compute P_F Faster

- Replace response (failure) surface with a surrogate model that is cheap to evaluate
  - Don't apply MCS to costly failure analysis
- Replace the physical model with a low-order model that is cheap to evaluate
  - Don't apply MCS to a costly physical model
- Perform the MCS in a more effective manner
  - Better sampling

30

Some Techniques

- Surrogate surfaces
  - Global approach: Polynomial Chaos Expansion (PCE)
  - Local approach: Cubic elements
  - Kriging and regression surfaces
  - B-Splines and Support Vector Machine (discontinuous behavior)
- Surrogate models: Proper Orthogonal Decomposition
- Sampling: Quasi Monte Carlo Simulation
- Applications: Linear and nonlinear airfoil, nonlinear panel, transonic wing

- **Giunta and Watson, "A Comparison of Approximation Modeling Techniques: Polynomial Versus Interpolating Models," AIAA 1998-4758.**
- **Chung and Alonso, "Using Gradients to Construct Cokriging Approximation Models for High-Dimensional Design Optimization Problems," AIAA 2002-0317.**
- **Millman, Maple, Beran, and Chilton, "Uncertainty Quantification with a B-Spline Stochastic Projection,"** ***AIAA Journal*****, Vol. 44, No. 8, 2006.**
- **Missoum, Beran, and Kurdi, "Reliability-Based Design Optimization of Nonlinear Aeroelastic Problems," AIAA 2008-2075.**

31

Polynomial Chaos Expansion (PCE)

- Use sampled data to develop a surrogate model
- Tailor spectral character to intended distribution
- Subject to the curse of dimensionality

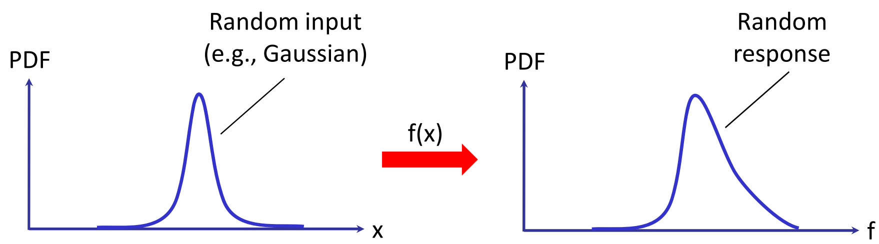

Goal: Quantify important characteristics of the distribution of f

32

PCE (cont.)

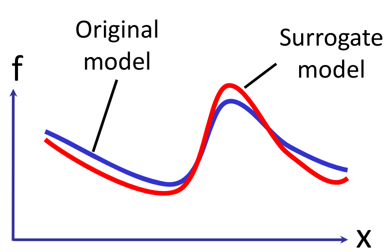

Spectral Approach: $f(x) \approx \sum_{i=1}^{M} F_i \Psi_i(x)$

- Complexity warrants N samples
- Construct accurate surrogate model with M components
- Desire M << N

Properties:

- Convergence: vary accuracy
- Orthogonality: find coefficients F_i
- Tailored: to improve properties

Ghanem and Spanos, Stochastic Finite Elements: A Spectral Approach, Springer, 1991

33

Two approaches to approximate f(x)

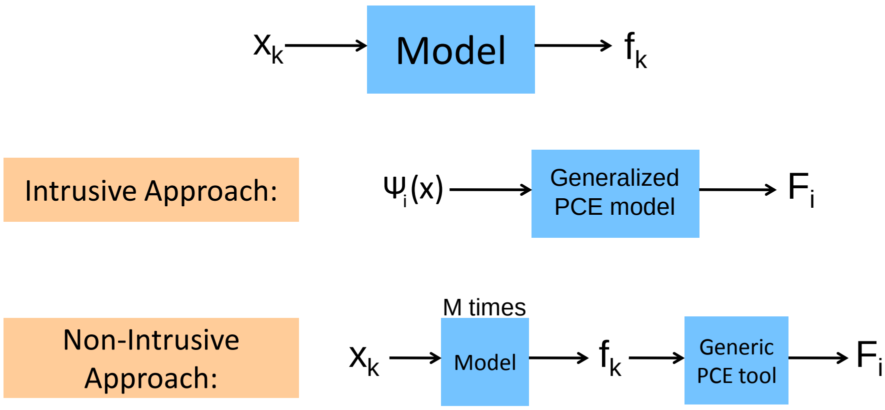

Non-intrusive approach minimizes new code development

Primary Types of Spectral Expansions

- Take more care to characterize the random input
  - x = x(ξ)
- Based on distributions of inputs and responses
  - Gaussian: Hermite polynomials
    - unbounded domain
    - select RVs that are normal
      - Zero mean and unit variance
  - Uniform: Legendre polynomials
    - bounded domain
  - Exponential: Laguerre polynomials
    - semi-bounded domain

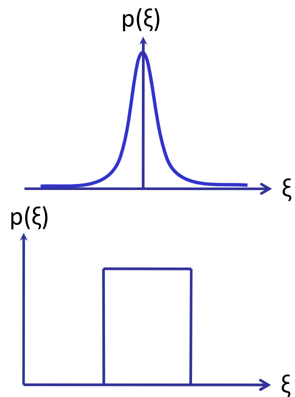

The Original Wiener-Hermite Form (1D)

Polynomial Forms

$$\Psi_i(\xi) = He_i(\xi) \quad (i = 0, \ldots)$$
$$\Psi_0(\xi) = 1$$
$$\Psi_1(\xi) = \xi$$
$$\Psi_2(\xi) = \xi^2 - 1$$
$$\Psi_{n+1}(\xi) = \xi\Psi_n(\xi) - n\Psi_{n-1}(\xi)$$

Orthogonality with respect to Gaussian measure

$$E[f] = \int_{-\infty}^{\infty} F_i\Psi_i(\xi)p(\xi)d\xi$$
$$< f, g >= E[fg] = \int_{-\infty}^{\infty} F_i\Psi_i(\xi)G_j\Psi_j(\xi)p(\xi)d\xi$$
$$\int_{-\infty}^{\infty} \Psi_i(\xi)\Psi_j(\xi)p(\xi)d\xi = 0 \quad (i \neq j)$$

Important formula for both intrusive and non-intrusive formulations →

$$< f, \Psi_j >= \int_{-\infty}^{\infty} F_i\Psi_i(\xi)\Psi_j(\xi)p(\xi)d\xi = F_i < \Psi_i^2 >$$

Hermite expansion leads to a very compact representation of the expected value of f →

$$< f, \Psi_0 >= F_0 = \int_{-\infty}^{\infty} fp(\xi)d\xi = E[f]$$

36

Non-Intrusive Point Collocation: Hosder et al.

2D Polynomial Forms

$$\Psi_0(\xi_1,\xi_2) = 1 \quad \Psi_3(\xi_1,\xi_2) = \xi_1^2 - 1$$
$$\Psi_1(\xi_1,\xi_2) = \xi_1 \quad \Psi_4(\xi_1,\xi_2) = \xi_1\xi_2$$
$$\Psi_2(\xi_1,\xi_2) = \xi_2 \quad \cdots$$

Least Squares (M>P+1)

$$SF = f \quad F = (S^TS)^{-1}S^Tf$$
$$M \approx 2(P+1) \quad \text{(optimal)}$$
$$\hat{S}_{1,2}F = f_{\xi_{1,2}} \quad \text{(w/sensitivities)}$$

M samples (structured or unstructured)

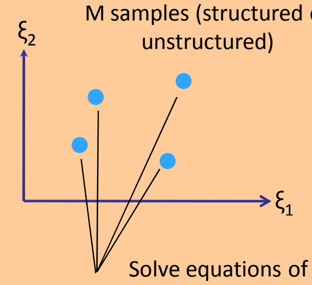

Solve equations of form:

$$\sum_{i=0}^{P} F_i\Psi_i(\xi_{1k},\xi_{2k}) = f_k \quad (k = 1, \ldots, M)$$

! $$P + 1 = \frac{(\dim + \text{order})!}{\dim!\,\text{order}!}$$

Hosder, Walters and Balch, "Efficient Sampling for Non-Intrusive Polynomial Chaos Applications with Multiple Uncertain Input Variables," AIAA 2007-1939

37

Test Case: Hosder Problem

$$F(X_1, X_2) = \ln(1 + X_1^2)\sin(5X_2)$$

$$\left.\begin{aligned} X_1 &= 2 + \sigma\xi_1 \\ X_2 &= 2 + \sigma\xi_2 \end{aligned}\right\}$$ **Monte Carlo samples**

ξ_1, ξ_2 Normal random variables

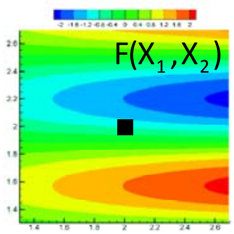

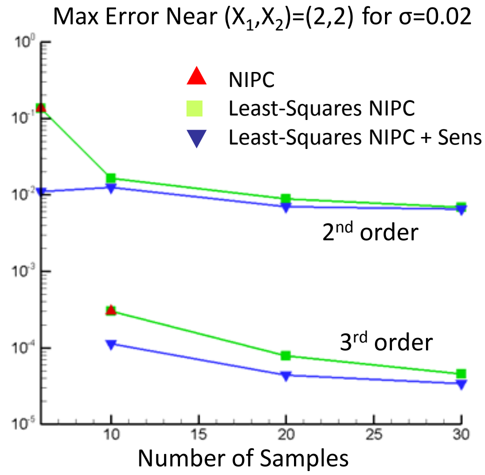

Infusion of sensitivities most effective for few samples

38

Application Case: Airfoil Problem

$$F(X_1, X_2) = \text{flutter surface}$$

$$\left.\begin{aligned} X_1 &= 100 + 10\xi_1 \\ X_2 &= 0.2 + 0.02\xi_2 \end{aligned}\right\}$$ **Monte Carlo samples**

ξ_1, ξ_2 Normal random variables

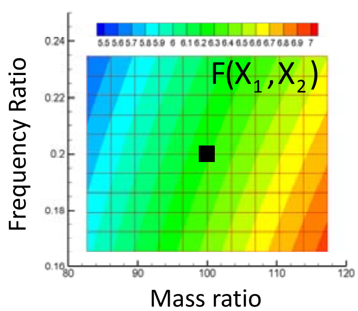

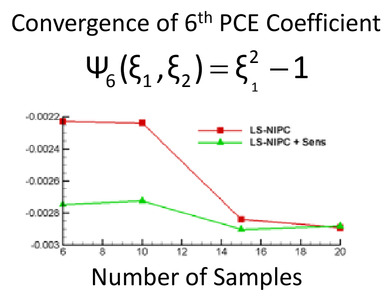

MCS Summary

($U_{critical}$ = 6, Gaussian, COV = 10%)

P_F=0.19:

- Physical airfoil model
- NIPC
- LS-NIPC
- LS-NIPC+Sens

39

Cubic Elements

- Local fitting approach that utilizes sensitivities
- System of global equations not required
- Subject to the curse of dimensionality

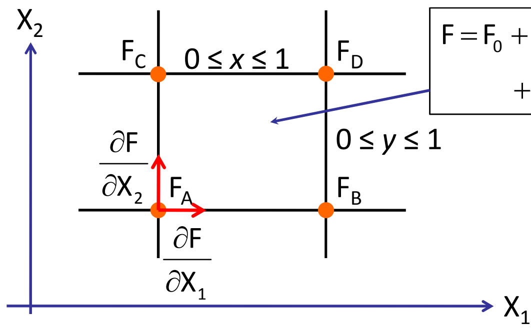

$$F = F_0 + F_1 x + F_2 y + F_3 xy + F_4 x^2 + F_5 y^2 + F_6 x^2 y + F_7 y^2 x + F_8 x^3 + F_9 y^3$$

Return to Hosder Case

$$F(X_1, X_2) = \ln(1 + X_1^2)\sin(5X_2)$$

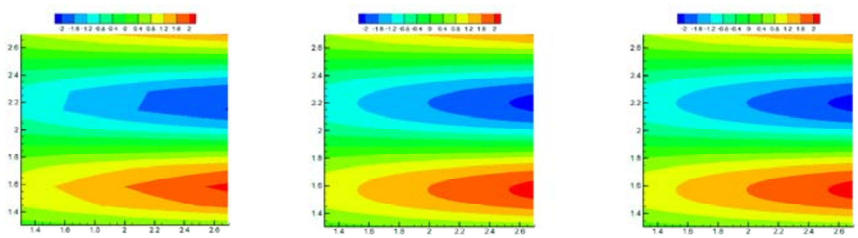

Sampling of F on 11 x 11 mesh

Surface fit of F on 321 x 321 mesh

Sampling of F on 321 x 321 mesh

Hosder Case (cont.)

Convergence verifies cubic formulation

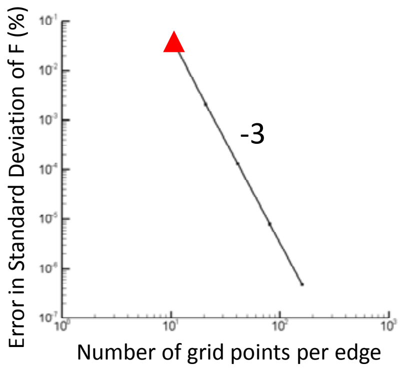

Comparison with PCE: ▲ Cubic

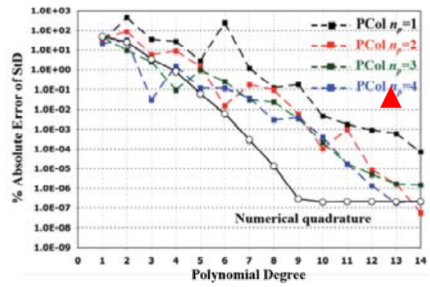

Hosder, Walters, and Balch, "Efficient Sampling for Non-Intrusive Polynomial Chaos Applications with Multiple Uncertain Input Variables," AIAA 2007-1939.

Cubic elements not as efficient as higher order global bases, but deliver accuracy with practicality

42

Linear Airfoil: Prediction of P_F

Goal: Determine P_F for flutter at specified reduced velocities

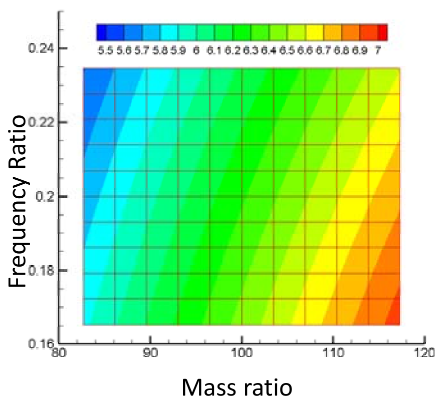

U_{fail} = 5.8

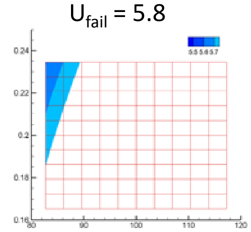

U_{fail} = 5.9

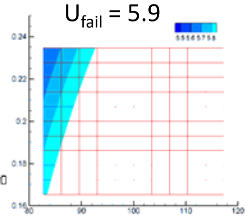

U_{fail} = 6.0

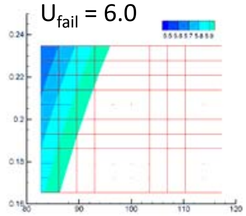

43

Linear Airfoil: MCS of Cubic Fit

(Random character of mass and frequency ratios: uniformly distributed with COV=10%)

P_F computation with 10^5 MCS samples

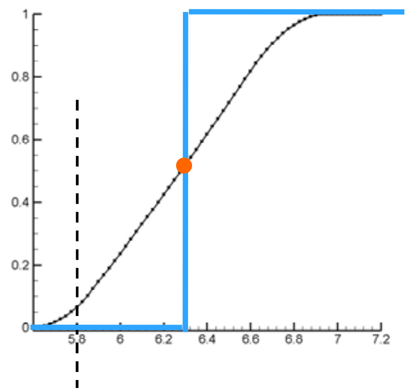

Convergence of MCS at U=5.8

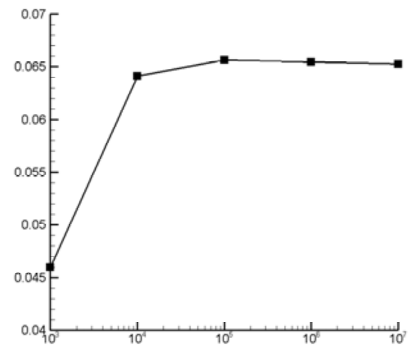

44

Extensions of Grid-Based Approach

Adaptive element refinement

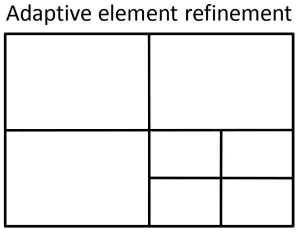

Non-simple domains

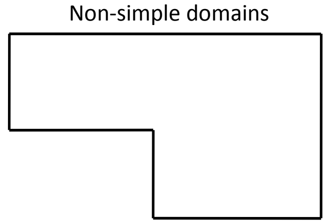

Hybrid formulations

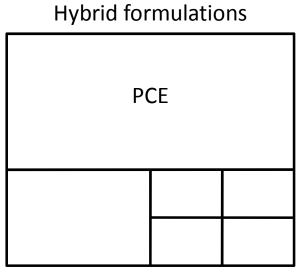

45

Transonic Airfoil

- Solution of Euler equations on a moderately sized grid
- Bifurcation calculation of the flutter speed (using Jacobian)
- O[10^4] DOFs
- Sensitivities computed with a direct method; favorably compared to perturbation analysis

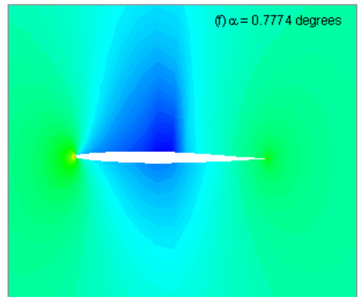

Beran and Morton, "A Continuation Method for the Calculation of Airfoil Flutter Boundaries," *JGCD*, Nov.-Dec., 1997

3D! **Badcock and Woodgate, "Prediction of Bifurcation Onset of Large Order Aeroelastic Models," AIAA 2008-1820**

Control! **Palaniappan, Sahu, Alonso, and Jameson, "Design of Adjoint Based Laws for Wing Flutter Control," AIAA 2009-0148**

Transonic Airfoil: Flutter Dip

Reduced Velocity

($U/b\omega_\alpha$)

Linear (Mach=0.0): U_F = 6.0
Euler (Mach=0.3): U_F = 6.3

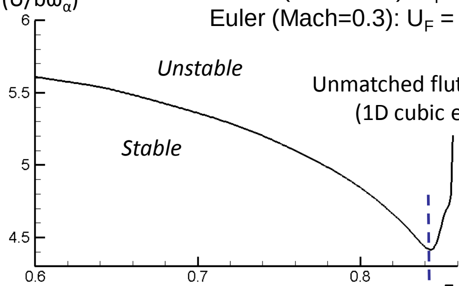

Unmatched flutter boundary (1D cubic elements)

Freestream Mach Number

Explore variations in mass ratio and frequency ratio at Mach 0.84

- Explored variations in Mach and pitch angle [1000 samples]:
  Hosder, Walters and Balch, "Efficient Uncertainty Quantification Applied to the Aeroelastic Analysis of a Transonic Wing," AIAA 2008-729.

Transonic Airfoil: Analysis in Dip

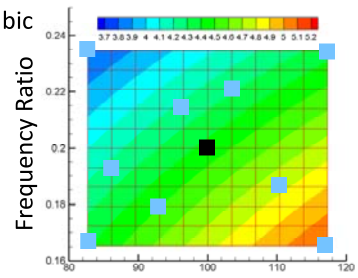

Nonlinearity in surface weak, but stronger than linear airfoil:
F_2 = 0.19; F_4 = -0.0042

Convergence of 4th PCE Coefficient

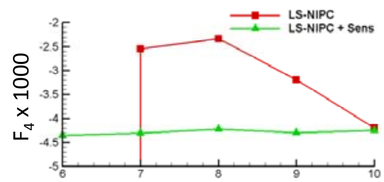

48

Application to Goland Wing

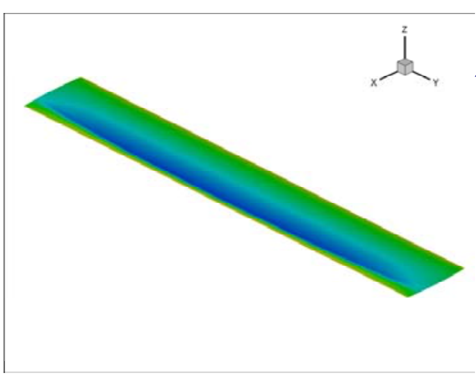

Mach 0.93 <u>with tip-store</u>
(Matched Analysis)

ZONA/ZEUS Nonlinear Dynamic Aeroelastic Analysis

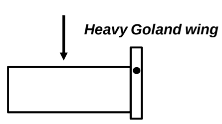

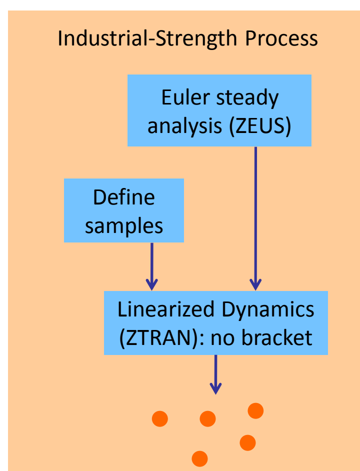

49

Goland Wing: Unmatched Euler-Based Analysis

Goal: Characterize responses for ensemble of 1000 wing structures

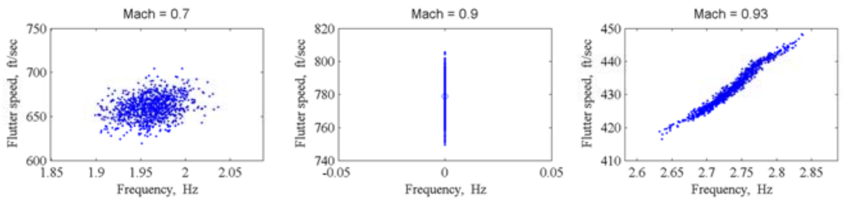

Interesting coherence in “flutter dip”

Kurdi, Lindsley and Beran, “Uncertainty Quantification of the Goland+ Wing’s Flutter Boundary, AIAA 2007-6309

50

Matched Analysis with PCE

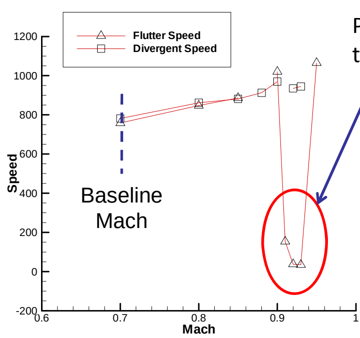

Precipitous “chimney” with high degree of sensitivity to damping; <u>verified sensitivity analysis</u>

Flutter altitude (2nd order PCE) as a function of upper and lower skin thickness

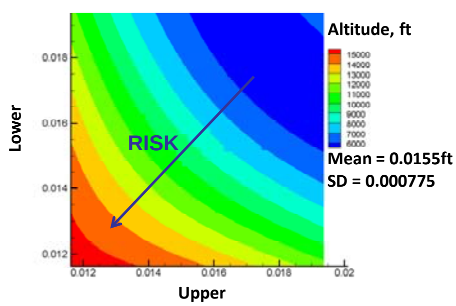

1000-sample mean altitude = 8704 ft
PCE mean (6 samples) = 8729 ft
1st term: $-839\xi_1$; 5th term: $41\xi_1\xi_2$

PCE enables stochastic interrogation with an “industrial-strength” process

51

What We Are Working On

Industrial-Strength Process

Euler steady analysis (ZEUS)

Define samples

Linearized Dynamics (ZTRAN): no bracket

Aeroelastic optimization, including maneuver

Gust analysis: Probabilistic and match filter theory

ROMs as F(M_∞, Altitude, AOA)

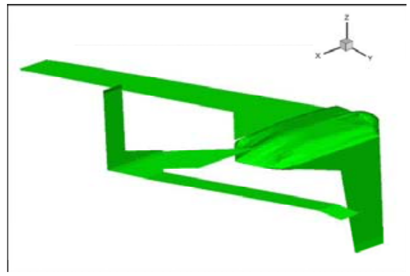

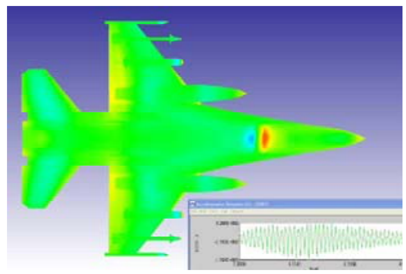

52

Panel in High-Speed Flow

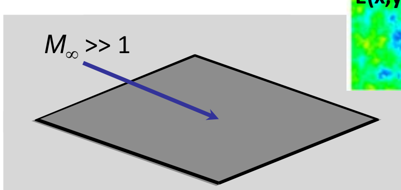

Simply supported von Kármán panel

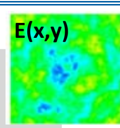

$$\lambda \propto \frac{\text{Dynamic Pressure (q)}}{\text{Stiffness (E)}}$$

How does variability in stiffness impact panel flutter speed (λ^*)?

- Formulate equations
- Compute flutter speed for a uniform panel: λ^*_0
- Use a spatially correlated MCS process to generate a set of random panels
- Linearly estimate flutter speed for each panel (k=1,…,N): λ^*_k
- Study worst cases and failure modes

53

Equations and Their Discretization

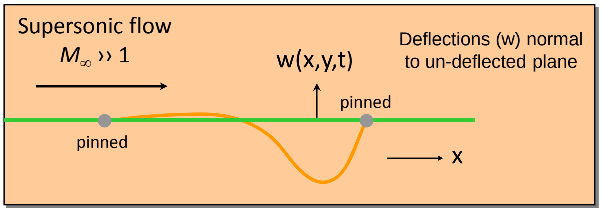

Piston Theory for pressure (p)

$$p = p\left(\frac{dw}{dx}, \frac{dw}{dt}\right)$$

- Relate local pressure to local changes in deflection
- Discretize 2nd-order structural equations with finite differences
- Uniform mesh (21 x 21)
- Place equations in 1st-order form: $Y = (W, dW/dt)^T$
- Stability comes from linearized equation:

$$\dot{Y} = J(\lambda)Y = \left(L_1 + \lambda^{-1}L_2\right)Y \qquad J(\lambda) = L_1 + \lambda^{-1}L_2$$

Lindsley, Beran, and Pettit, "Integration of Model Reduction and Probabilistic Techniques with Deterministic Multi-Physics Models," AIAA 2006-0192.

54

Stochastic Viewpoint

$$J = L_1 + \left[\frac{1}{\Lambda(x,y)}\right]L_2 \quad \Longleftarrow \quad \lambda \propto \frac{\text{Dynamic Pressure (q)}}{\text{Stiffness (E)}}$$

Panel-specific Jacobian

$$J(\lambda, D_k) = L_1 + \left[\frac{1}{\lambda}\right]D_k L_2$$

L_1 and L_2 invariant

Variability matrix

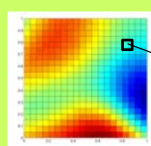

$E(x_i, y_j)/E_0$

$D_k = [\ddots]$

- λ defined in terms of uniform panel: $\lambda \propto q/E_0$
- D expresses variability in E normalized by the uniform panel
- Flutter speed of uniform and imperfect panel: λ_0^* & λ_k^*

55

Modeling Variability in Stiffness

Goals: (1) Simulate a process that generates a random distribution E(x,y) that is spatially correlated*; (2) use sensitivity analysis to predict distribution of flutter speeds

Ensemble of 1000 panels with variability in frequency and phase (COV≈5%)

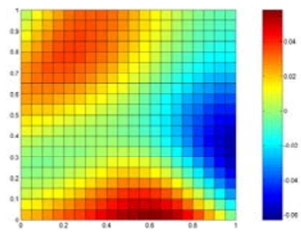

Histogram of variations in parameter λ (match full order)

$$\frac{\delta\beta}{\delta\lambda} = \left[\frac{1}{q^* z}\right]\left[q^* \frac{\delta J}{\delta\lambda} z\right]$$

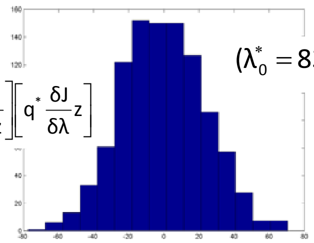

$(\lambda_0^* = 833)$

*Deodatis, "Stochastic FEM Sensitivity Analysis of Nonlinear Dynamic Problems," Prob. Mech Eng., 4(3), 1989

56

Model Reduction

$$\delta\beta = \mathbf{q}^* \delta J \mathbf{z} / \mathbf{q}^* \mathbf{z} \Leftarrow \begin{array}{l} \mathbf{z}^*_{\mathrm{ROM}} = \Phi \hat{\mathbf{z}}^*_{\mathrm{ROM}} \\ \mathbf{q}^*_{\mathrm{ROM}} = \Phi \hat{\mathbf{q}}^*_{\mathrm{ROM}} \end{array}$$

Model reduction through Proper Orthogonal Decomposition (POD)

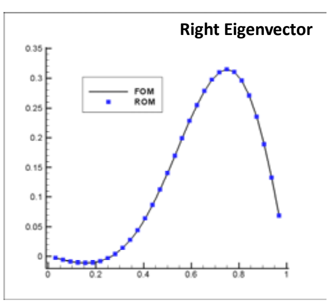

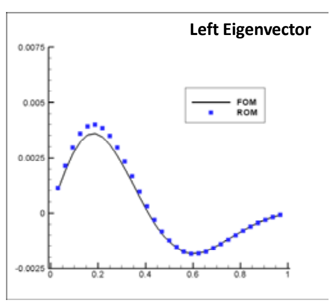

$\mu = 0.1$	
$\lambda^* =$ 8073.6	(direct)
$\lambda^* =$ 8073.5	(ROM)

$\mu = 0.101$	
$\lambda^* =$ 7993.9	(direct)
$\lambda^* =$ 7992.4	(FOM perturbation)
$\lambda^* =$ 7992.3	(ROM perturbation)

57

Low Discrepancy Sampling (LDS)

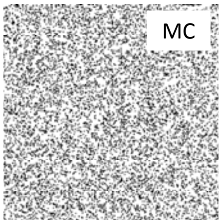

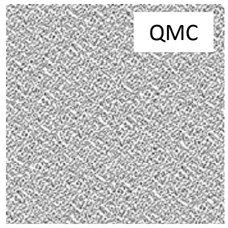

Use mathematical sequences to generate more evenly distributed samples: Quasi-Monte Carlo

Camberos, Greendyke, and Lambe, "On Direct Simulation Quasi-Monte Carlo Methods," AIAA 2008-3915

Integral of sin(xy) in 2D

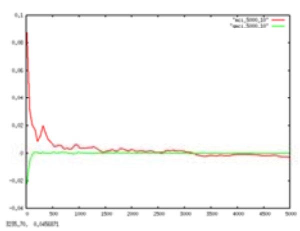

Boltzman Collision Integral in 5D

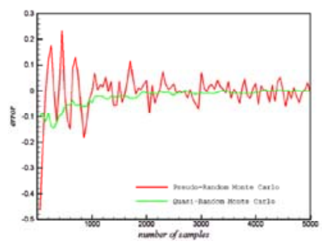

Can P_F (non-smooth integral) be computed faster with QMC in high-dim?

58

Summary

- Many techniques exist for uncertainty quantification (UQ) that can be applied to aeroelastic systems
- However, aeroelasticity poses certain challenges
  - Long run times for physics-rich problems
  - Problem of precisely determining flutter speed
  - Goal: minimize amount of sampling
- Direct flutter methods are fast & minimize sampling
- Sensitivities to key parameters should always be computed
- These sensitivities can be used to improve UQ techniques

59

Linear Airfoil: First-Order Reliability Method (FORM)

- Normalize: $\mu / \mu_{baseline} \rightarrow \mu'$; $\omega / \omega_{baseline} \rightarrow \omega'$

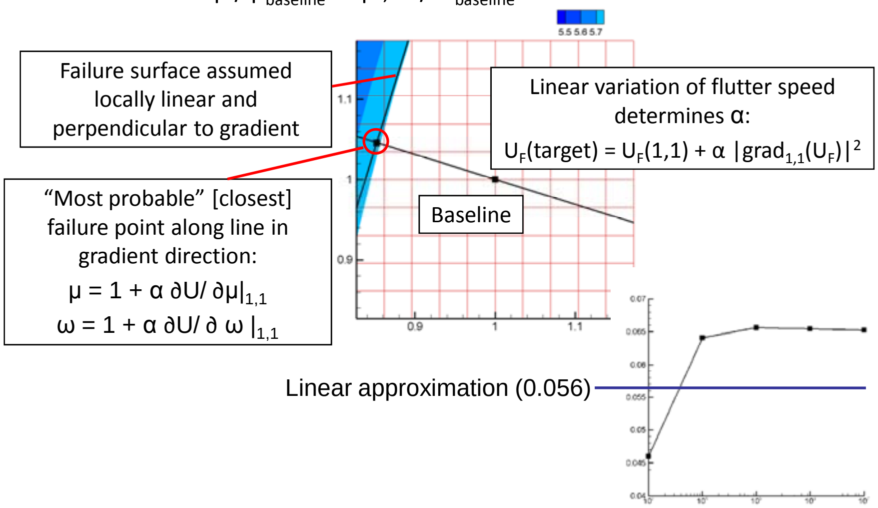

60

Roadmap

← Predict

→ Manage

P_F ← **Flutter Identification** ← **Modal Uncertainty** ← **Element Uncertainty**

Probability of Failure
- **Indirect**
  - Response surface
  - Support Vector Machine
  - Monte Carlo Simulation
- **Direct**
  - Kriging and co-Kriging
  - Polynomial Chaos Expansions
  - Monte Carlo Simulation

Flutter ID
- **Indirect**
  - Brackets
  - Finite-difference sensitivities
  - Black box
- **Direct**
  - Bifurcation (linearized)
  - Adjoint sensitivities
  - Specialized

61

Worst-case Scenario

Goal: Identify worst-case stiffness distribution & ensure panel safety is robust

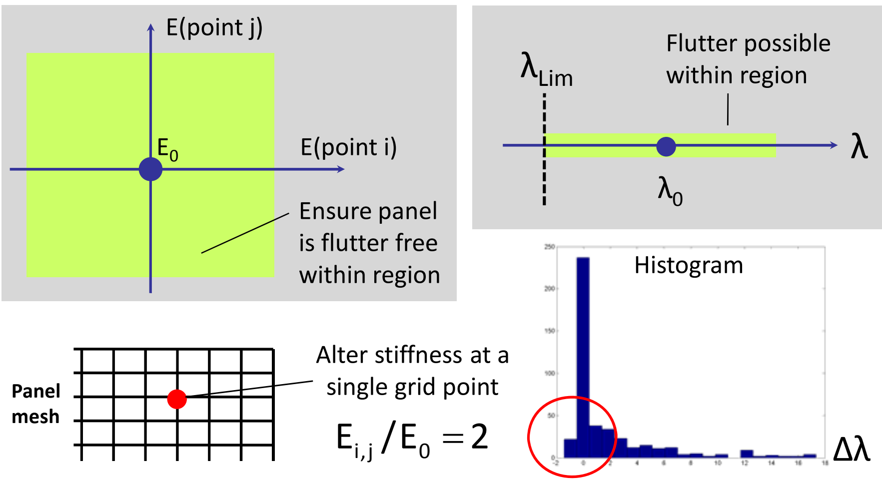

62

Worst-case Scenario (cont.)

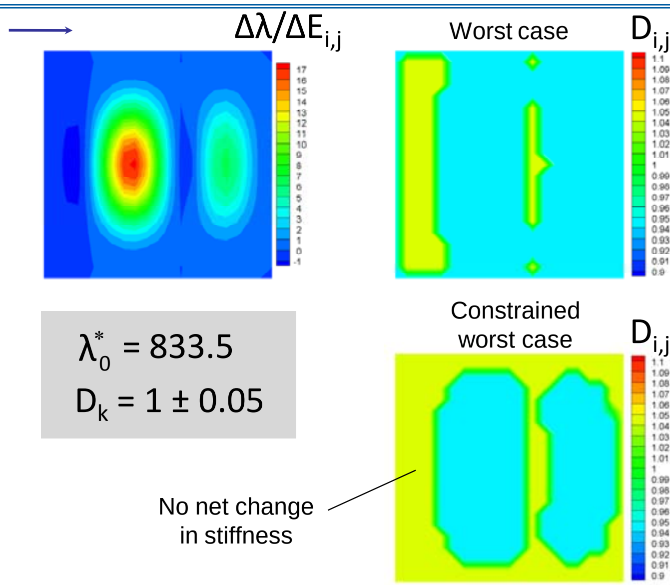

λ^*_0 = 833.5

D_k = 1 ± 0.05

$\Delta\lambda^*_k$ = -44.88

(5.4% decrease)

$\Delta\lambda^*_k$ = -44.58

(5.3% decrease)

63

Stochastic Viewpoint (cont.)

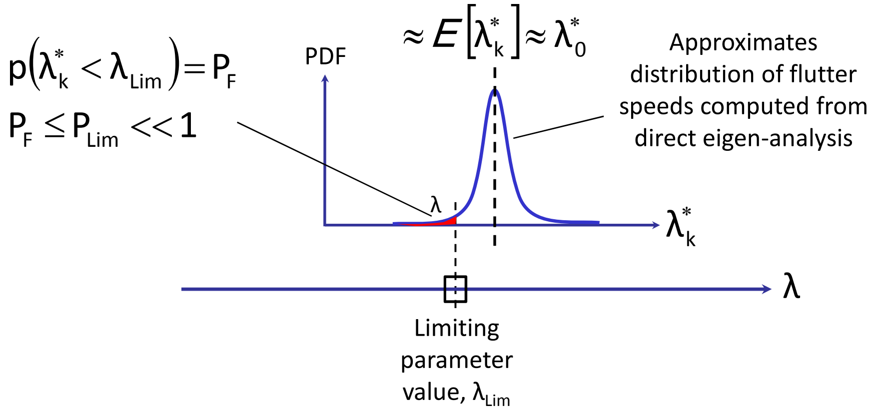

Evaluate $P_F = P_F(\lambda_{Lim}, \lambda)$